Human Reproduction, Vol.28, No.12 pp. 3271–3282, 2013
Advanced Access publication on October 15, 2013 doi:10.1093/humrep/det381

human reproduction

ORIGINAL ARTICLE *Reproductive biology*

Mechanistic foundations of the metaphase II spindle of human oocytes matured *in vivo* and *in vitro*

Giovanni Coticchio[1,*], Maria Cristina Guglielmo[1], Mariabeatrice Dal Canto[1], Rubens Fadini[1], Mario Mignini Renzini[1], Elena De Ponti[2], Fausta Brambillasca[1], and David F. Albertini[3]

[1]Biogenesi Reproductive Medicine Centre, Istituti Clinici Zucchi, Via Zucchi 24, Monza, Italy [2]Department of Medical Physics, San Gerardo Hospital, Monza, Italy [3]Department of Molecular and Integrative Physiology, University of Kansas, Kansas City, USA

*Correspondence address. Tel: +39-039-8383314; Fax: +39-039-8383369; E-mail: coticchio.biogenesi@grupposandonato.it

Submitted on May 23, 2013; resubmitted on September 3, 2013; accepted on September 17, 2013

STUDY QUESTION: Are morphometric and morphological parameters of the metaphase II (MII) spindle of human oocytes matured *in vivo* or *in vitro* predictive of chromosome alignment on the metaphase plate?

SUMMARY ANSWER: Morphometric spindle parameters were very comparable between oocytes matured *in vivo* and *in vitro* and were unable to predict chromosome alignment, while a flattened shape of both poles was positively associated with chromosome displacement from the metaphase plate.

WHAT IS KNOWN ALREADY: The relationship between MII spindle morphometry and chromosome alignment has only been sporadically investigated in human oocytes. The possible implications of spindle pole morphology are totally unrecognized.

STUDY DESIGN, SIZE, DURATION: Morphometric and morphological analysis of the MII spindle of donated supernumerary human oocytes ($N = 93$) aimed at investigating possible associations between novel microtubule parameters and chromosome arrangement.

PARTICIPANTS/MATERIALS, SETTING, METHODS: MII oocytes from three sources were analysed: (i) stimulated cycles matured *in vivo* (ivo-MII), (ii) leftover cumulus-free germinal vesicle oocytes from stimulated cycles matured *in vitro* (lgv-MII) and (iii) immature cumulus-cell oocyte complexes (COCs) recovered from *in vitro* maturation (IVM) cycles and matured *in vitro* (ivm-MII). Oocytes were fixed and stained for tubulin, chromatin and actin. Optical sections were collected at 0.3 μm intervals by high-performance confocal microscopy and three-dimensionally reconstructed for assignment of specific spindle and chromosomal properties. Spindle pole morphology was classified as either focused or flattened depending on whether microtubule ends were more or less convergent, respectively. Optical density measurements were generated to estimate microtubule abundance in chromosome to pole domains proximal and distal to the oolemma.

MAIN RESULTS AND THE ROLE OF CHANCE: In ivo-MII oocytes, the sizes (mean ± SD) of major and minor axes were 11.8 ± 2.6 and 8.9 ± 1.7 μm, respectively, while maximum projection was 88.8 ± 29.5 μm^2. Very comparable values of these parameters were found in lgv-MII and ivm-MII oocytes. Double-focused spindles were rarely found (3.1%), unlike those with a double-flattened conformation (47.7%). Spindles with both focused and flattened poles amounted to almost half of the sample set (49.2%), but in this subgroup it was very infrequent (4.6%) to observe the flattened pole oriented towards the oolemma. Overall, differences in the relative proportions of pole morphology categories in ivo-MII, lgv-MII and ivm-MII oocytes were not statistically significant. For both the distal and proximal spindle hemidomains, optical intensity profiles were also comparable between ivo-MII, lgv-MII and ivm-MII oocytes. None of the morphometric parameters (major and minor axes, their ratio, maximum projection, distances of the metaphase plate from the poles) was associated with chromosome alignment on the metaphase plate or arrangement inside and outside the spindle. Importantly, a double-flattened outline of pole morphology was positively associated with the displacement of one or more chromosomes from the metaphase plate. Moreover, when a flattened pole was oriented towards the oolemma, a higher rate of chromosome displacement was observed.

LIMITATIONS, REASONS FOR CAUTION: The findings of the study will require confirmation by further in-depth analysis and extension of the database, especially regarding the relationship between microtubule abundance and chromosome arrangement. Furthermore, considering the high number of comparisons, the observed statistical differences will require future '*ad hoc*' analysis.

WIDER IMPLICATIONS OF THE FINDINGS: Collectively, this work provides a robust database for future research on the human oocyte cytoskeleton, and contributes to a better definition of oocyte quality in assisted reproduction technology. Also, these data support the notion that IVM does not affect spindle morphometry and morphology.

STUDY FUNDING/COMPETING INTEREST(S): Part of this work was supported by a grant awarded by the Italian Ministry of Labour, Health and Social Policies. The authors have no conflicts of interest to declare.

TRIAL REGISTRATION NUMBER: Not applicable.

Key words: oocytes / cytoskeleton / spindle / chromosomes / meiosis

Introduction

The metaphase I (MI) and II (MII) spindles are central to the completion of oocyte meiosis, subserving the process of chromosome segregation. Their position ensures that the cleavage furrow plane of the two meiotic divisions lays cortically, minimizing loss of ooplasm during emission of polar body I (PBI) and II (PBII) (Brunet and Verlhac, 2010). The significance of spindle function for oocyte quality and, ultimately, the outcome of assisted reproduction technology (ART) treatment has long been recognized. For example, it is widely held that defects in MII spindle morphology and chromosome alignment contribute to or are predictive of the increased prevalence of aneuploidy observed in oocytes of older aged women (Battaglia *et al.*, 1996). Moreover, extrinsic factors, such as inappropriate culture conditions (Pickering and Johnson, 1987; Wang *et al.*, 2002) or cryopreservation (Coticchio, 2006; Bromfield *et al.*, 2009; Coticchio *et al.*, 2009), disrupt spindle organization, with predictably detrimental consequences on oocyte quality. However, our understanding of the relationship between the structure of the meiotic spindle and its function remains poor.

In mammalian oocytes, the MII spindle is generically described as a symmetrical barrel-shaped structure formed from bundles of microtubules on which chromosomes are equatorially aligned in preparation for chromatid disjunction and segregation. In reality, the MII spindle of the human oocyte exhibits a variety of structural manifestations that, while complying with the classical bipolar organization, can differ substantially from one another and with uncertain functional significance. For example, little is known of possible relationships between spindle size—length, width, volume—and function. This has potentially important implications for human IVF because animal models suggest the existence of an association between spindle geometry and the fidelity of the processes of chromosome segregation and PBII extrusion (Sanfins *et al.*, 2003). In the humans, other morphological aspects of the MII spindle have not been explored and remain totally unappreciated. Microtubules minus ends may converge closely, forming focused spindle poles. Alternatively, they may be more loosely held together and give rise to flattened spindle terminals. Spindles may appear similar in their typical bipolar outline and yet have considerably different mass, being formed from bundles of microtubules of different thickness. Chromosomes may be orderly aligned on the equatorial plate, but differentially distributed between the inside and outside of the spindle surface (Bromfield *et al.*, 2009; Coticchio *et al.*, 2009). These and other aspects deserve an effort of understanding, considering their potential influence on the mechanics of meiosis.

Here, we aimed at answering some of these questions, to provide a robust database of the cytoskeleton of the mature oocyte to define more objectively human oocyte quality in ART and contribute to the progress of present and future treatments, such as oocyte *in vitro* maturation (IVM), oocyte cryopreservation and nuclear genome transfer. To this end, a rigorous and reproducible confocal microscopy morphometric analysis was carried out on human oocytes matured *in vivo* or *in vitro*, with special emphasis on spindle organization and chromosome disposition. Collectively, our data shed new light on the MII spindle and cast novel perspectives for future research on the mechanics of chromosome segregation in the human oocyte.

Materials and Methods

Source of oocytes

Ninety-three supernumerary oocytes were obtained from 70 consenting women undergoing assisted reproduction treatment for various causes of infertility (male factor, tubal factor, stage I/II endometriosis or unexplained infertility). Mean ± SD female age was 35.6 ± 4.3 years (range 26–43). A maximum of four oocytes were donated *per* woman.

Oocytes derived from controlled ovarian stimulation cycles

Pituitary down-regulation was achieved by gonadotrophin-releasing hormone agonist (Decapeptyl 3.75 mg or 0.1 mg, Ipsen, Italy). Stimulation of follicle growth was carried out with rFSH (Merck Serono, Rome, Italy or Schering Plough, Italy), tailoring doses and duration of stimulation according to patient characteristics (Fadini *et al.*, 2009). Ten thousand IU of hCG were administered 36–38 h prior to oocyte collection. After retrieval, oocytes were cultured in Universal IVF medium (Origio, Måløv, Denmark). Within 3 h from collection, cumulus cells were removed by brief exposure to culture medium containing cumulase (80 U/ml; Origio, Måløv, Denmark), followed by mechanical action achieved by passage through a fine bore pipette. Surplus donated oocytes were destined to different treatments depending on their stage of development. Oocytes displaying the PBI were immediately fixed and stored at 4°C for subsequent staining and confocal analysis. Immature denuded germinal vesicle (GV) stage oocytes were transferred to microdrops of IVF medium (Origio, Måløv, Denmark) and incubated at 37°C in a 6% CO_2 humidified atmosphere. After 30 h, oocytes showing the PBI were fixed and stored at 4°C for subsequent staining and confocal analysis.

Oocytes obtained from IVM cycles

In IVM cycles, patients were primed with 150 IU/day FSH for 3 days from Day 3 of the cycle. All women were monitored for follicular growth until a leading follicle of 10–12 mm in diameter and an endometrial thickness >5 mm were observed. Under those conditions, oocyte retrieval was scheduled to occur after 36–38 h from hCG (10 000 IU) administration.

Follicle aspiration was performed under transvaginal ultrasound guidance using a single lumen aspiration needle (code 4551-E2 Ø17, gauge 35 cm; Gynetics, Lommel, Belgium) connected to a vacuum pump (pressure 80–100 mmHg; Craft Pump, Rocket Medical, Washington, UK). Follicular aspirates containing cumulus cell-oocyte complexes (COCs) were collected in a single 50 ml tissue culture flask containing 15 ml of pre-warmed Flushing Medium with heparin (Origio, Måløv, Denmark). Follicular aspirates were filtered through a 70 μm cell strainer (Becton-Dickinson, Buccinasco, Italy) and washed twice with Flushing Medium. COCs were detected under a stereomicroscope and thoroughly washed.

COCs were examined and classified according to cumulus oophorus morphology and stage of oocyte maturation. Surplus donated COCs including a GV-stage oocyte surrounded by multiple layers of cubical and tightly compacted cumulus cells were selected for culture and subsequent analysis.

IVM

After recovery, COCs were transferred to a single well Petri dish containing 0.5 ml of IVM medium (Vial 2 of IVM system medium; Origio, Måløv, Denmark) supplemented with 75 mIU/ml recombinant FSH (Merck Serono, Rome, Italy), 100 mIU/ml hCG (Merck Serono, Rome, Italy) and 4% human serum albumin (Baxter, Vienna, Austria). Culture was carried out at 37°C in a 6% CO_2 humidified atmosphere for 30 h. Afterwards, COCs were treated enzymatically and mechanically to remove cumulus cells, as described above. Oocytes showing the PBI were fixed and stored at 4°C for subsequent staining and confocal analysis.

Oocyte fixation and immunostaining

Oocytes were fixed in microtubule-stabilizing buffer (100 mM PIPES, 5 mM MgCl2, 2.5 mM EGTA, 2% formaldehyde, 0.1% Triton-X-100, 1 mM taxol, 10 U/ml aprotinin and 50% deuterium oxide) for 30 min at 37°C and stored in blocking solution (0.2% sodium azide, 2% normal goat serum, 1% BSA, 0.1 M glycine and 0.1% Triton X-100 in PBS) at 4°C until further processing. After storage in blocking solution (for a few weeks maximum), oocytes were further processed for immunostaining, through serial incubations with primary and secondary antibodies (1 h per antibody at 37°C with shaking) followed by washing (three washes of 15 min) in blocking solution after each antibody incubation. Microtubule staining was performed by using a mouse monoclonal anti-α/β tubulin antibody mixture (Sigma Biosciences, Italy) diluted 1:100 in wash solution, followed by exposure to Alexa 488 goat anti-mouse IgG (1:500; Molecular Probes, USA). Rhodamine-phalloidin (1:200; Molecular Probes, USA) and Hoechst 33 258 (1 μg/ml, Molecular Probes, USA) were used to detect actin and chromatin, respectively. Finally, samples were mounted in medium containing 50% glycerol, 25 mg/ml sodium azide and 1 μg/ml Hoechst 33 258 using wax cushions to avoid compression of samples.

All possible measures were taken to make signal intensity and patterns comparable between samples analysed by confocal microscopy at different times during the period of study. While samples were fixed at different times, freshly prepared MTSB-XF fixative was always used. Samples were fixed for precise intervals (30 min at 37°C) and stored in the same blocking solution (at 4°C) prior to processing and imaging. In addition the following potential variables were controlled as follows:

(i) The confocal microscopy apparatus was subject to regular checks by the staff of the microscopy facility (Alembic, Milan, Italy) to confirm repeatability of signal emission generated by a reference sample analysed under identical acquisition conditions.
(ii) To assure antibody access and specificity and therefore enhance measure repeatability, priority was given to some factors:
  (a) Once samples were fixed, they were subject to a conditioning step that assured cessation of any residual fixation and included a buffer whose composition was designed to maximize blocking of spurious antibody binding prior to exposure to primary antibody.
  (b) Such solutions were also used to prepare primary and secondary antibodies. This met the stringent requirements required for optimal antigen–antibody complex formation and reducing background.
(iii) Sample were fixed at different times and stored for a few weeks at 4°C, but primary and secondary antibody exposures were performed the day before each confocal microscopy acquisition session.
(iv) Image acquisition was carried out under identical instrumental conditions in each confocal microscopy session.

Image acquisition and analysis

Labelled oocytes were analysed using a Leica TCS SP2 Laser Scanning Confocal microscope equipped with a 63× objective and KrArg (488 nm excitation) and HeNe (543 nm excitation) lasers for collection of complete three channel Z-stacks through the entire spindle of each oocyte. Optical sections were collected at 0.3 μm intervals and reconstructed three dimensionally for assignment of specific spindle and chromosomal properties (Supplementary data, Fig. S1A and B). Spindles were analysed according to one- and two-dimensional characteristics using LCS Lite software in *X*, *Y* or *Z* planes so that measurements could be calculated in oocytes regardless of spindle orientation. The following morphometric parameters were measured for each spindle: (i) major axis, (ii) minor axis, (iii) distance of poles from the metaphase plate and (iv) area of maximum projection. Maximum projection was defined as the 2D area represented by the reconstruction of *Z* axis data sets into a 3-D representation of the total pixel array for each spindle, irrespective of the original orientation within each oocyte. The shape of spindle poles proximal and distal to the oocyte surface was classified as flattened or focused. Flattened poles were defined as ones having an overall size of 2 μm or more, whereas focused poles were defined as those having an overall size of <2 μm.

Each spindle was further characterized based on whether all chromosomes were aligned on the metaphase plate or if chromosomes were misaligned. Misalignment was denoted as any case where there was ≥ 2 μm displacement of at least one chromosome from the metaphase/equatorial plate. Chromosome arrangement inside and outside the spindle surface was also evaluated. In reconstructions from a polar angle, we defined chromosome disposition as being normal when two sets of concentric arrays were apparent or if there was deviation from this, as indicated by peripheral displacement or absence of a complete inner ring, they were classified as abnormal.

In each spindle, microtubule density was assessed by detecting tubulin staining from full reconstructions of *Z*-plane data sets. By using LCS Lite software, optical intensity profiles for the tubulin channel were measured along two lines drawn in an intermediate position between the pole and the metaphase plate in each spindle half.

After subtraction of background, tubulin staining parameters were expressed as arbitrary units. For both the distal and proximal hemispindles, the following parameters were measured: (i) peak of maximum intensity, (ii) mean intensity of peaks, (iii) fibre intensity, i.e. the ratio between mean intensity and number of peaks of each set. Peaks were identified as the highest isolated values of each line scan, without including minor spikes. In addition, independent observation by two operators assured consistency of peak identification.

Statistical analysis

Absolute and percentage frequencies were used to describe categorical items while mean values, standard deviation and minimum-to-maximum range were used for continuous variables. To analyse differences between groups, Student's *t*-test, Kruskal–Wallis rank test and Fisher's exact test

were used, for normally and not-normally distributed continuous variables and for categorical characteristics, respectively.

Stata software 9.0 (Stata Corporation, College Station, Texas, USA) was used for performing statistical analysis and a level of $P < 0.05$ was adopted for significance. No correction was made to account for the high number of comparisons.

Results

This study documents a morphometric analysis of the MII spindle of human oocytes obtained from controlled ovarian stimulation cycles and matured *in vivo* (ivo-MII). For comparison, two other classes of oocytes were also analysed: (i) oocytes matured *in vitro* from leftover cumulus-free GV oocytes (lgv-MII) derived from controlled ovarian stimulation cycles and (ii) oocytes matured *in vitro* from immature cumulus cell-oocytes complexes (ivm-MII) derived from IVM cycles. The relative proportions of ivo-MII, lgv-MII and ivm-MII oocytes were 63.4% ($n = 59$), 25.8% ($n = 24$) and 10.8% ($n = 10$), respectively.

Spindle morphometry and geometry

Spindle morphometric parameters (Fig. 1) are reported in Table I. In ivo-MII oocytes, sizes (mean ± SD) of major and minor axes were 11.8 ± 2.6 and 8.9 ± 1.7 μm, respectively, while maximum projection was 88.8 ± 29.5 μm^2. The metaphase plate was not perfectly equatorial, but slightly shifted towards the pole proximal to the oocyte surface. The characteristics of lgv-MII and ivm-MII oocytes were very similar, with the exception of the major/minor axis ratio that was smaller in spindles of lgv-MII oocytes.

In all samples, spindle distance (mean ± SD) from the oocyte surface (Fig. 1), identified by cortical actin, was 7.0 ± 7.7 μm (range 1.6–36.8). This parameter was comparable between the three classes of oocytes (data not shown).

Spindle pole morphology was described as either focused or flattened depending on whether minus ends of microtubules were more or less convergent, respectively (Fig. 2A–D). Double-focused spindles were rarely found (3.1%), unlike those with a double-flattened conformation (47.7%). Spindles with both focused and flattened poles amounted to almost half of the sample set (49.2%), but in this subgroup it was very infrequent (4.6%) to observe the flattened pole oriented towards the oolemma. Overall, differences in the relative proportions of pole morphology categories in ivo-MII, lgv-MII and ivm-MII oocytes were not statistically significant (Table II). However, spindles with flattened poles oriented towards the oolemma were more frequently represented in lgv-MII oocytes, in comparison with ivo-MII and ivm-MII oocytes (78.3, 46.9 and 40.0%, respectively, $P = 0.036$; data not shown in table).

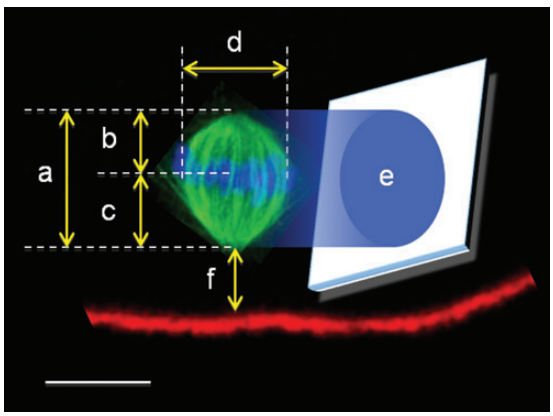

Figure 1 Metaphase II spindle morphometric parameters after three-dimensional reconstruction from individual optical sections. Microtubule tubulin is represented in green, chromosomes in blue and actin in red. (a) Major axis; (b) distal pole, metaphase plate distance; (c) proximal pole, metaphase plate distance; (d) minor axis; (e) maximum projection and (f) proximal pole, cortex distance. Bar equals 10 μm.

Optical intensity profiles for the tubulin channel were generated to estimate microtubule abundance. This was achieved by acquiring signal intensity along two reference lines transecting the spindle halves (hemidomains), proximal and distal to the oocyte surface, in an intermediate position between the pole and the metaphase plate. The following intensity parameters were taken into account: peak of maximum intensity, overall mean intensity and microtubule bundle intensity (Fig. 3, see also Materials and Methods). These parameters, for both the distal and proximal spindle hemidomains, were comparable between ivo-MII, lgv-MII and ivm-MII oocytes (Table III).

Spindle characteristics and chromosome arrangement

Possible associations between the above morphological parameters and chromosome arrangement were investigated. As we did not apply kinetochore markers for discriminating between homologues and sister chromatids, we restricted our use of the term chromosome to include either of these forms of meiotic chromosomes. Here, the above parameters regarding the spindle were studied in relation to the disposition of chromosomes. Two perspectives for chromosome disposition were evaluated. In lateral view of the spindle, we recorded whether all chromosomes were organized within a metaphase plate (aligned, Supplementary data, Fig. S2A) or when a single chromosome or more were displaced from the plate by at least 2 μm (misaligned, Supplementary data, Fig. S2B). None of the morphometric parameters (major and minor axes, their ratio, maximum projection, distances of the metaphase plate from the poles) was associated with the alignment of all chromosomes on the metaphase plate or the displacement of one or more of them towards the poles (Table IV). In a second perspective, afforded in situations where a complete Z-stack allowed reconstruction from a polar angle, we defined chromosome disposition as being normal when two sets of concentric arrays were apparent (Fig. 4A) or if there was deviation from this, as indicated by peripheral displacement or absence of a complete inner ring, they were classified as abnormal (Fig. 4B). It is important to note that in some circumstances in which it was possible to acquire both a lateral and polar view of the same spindle, a lateral alignment (Fig. 1) was found to coincide with a polar view showing concentric/normal alignment (Fig. 4A), while in other cases a lateral alignment (Fig. 2A) was associated with a polar misalignment (Fig. 4B). Based on this parameter, no correlation emerged between these two alternative chromosome configurations and spindle morphological characteristics (Table V).

A double-flattened outline was positively associated with the displacement of one or more chromosomes from the metaphase plate (Table VI). The orientation of a flattened, instead of focused, pole

Table I Spindle morphometry in MII oocytes matured *in vivo* or *in vitro*.

Parameter	All oocytes	Oocyte category (*n*)			*P*
		ivo-MII (59)	Igv-MII (24)	ivm-MII (10)	
Major axis (μm)	11.6 ± 2.3 (7.2–18.9)	11.8 ± 2.6 (7.3–18.9)	11.1 ± 1.7 (7.2–13.6)	12.0 ± 2.3 (7.7–15.9)	0.399
Minor axis (μm)	9.0 ± 1.6 (3.4–12.9)	8.9 ± 1.7 (3.4–12.9)	9.4 ± 1.2 (7.4–11.6)	8.6 ± 1.5 (6.3–10.5)	0.291
Major/minor axis ratio	1.32 ± 0.32 (0.74–2.81)	1.36 ± 0.35 (0.74–2.81)	1.19 ± 0.19 (0.89–1.48)	1.44 ± 0.36 (0.86–1.96)	0.042
Maximum projection (μm^2)	89.0 ± 25.8 (29.1–167.9)	88.8 ± 29.5 (29.1–167.9)	87.2 ± 17.8 (44.8–116.7)	94.7 ± 18.1 (66.5–122.8)	0.744
Proximal pole, met. plate (μm)	5.5 ± 1.3 (3.2–9.7)	5.5 ± 1.5 (3.2–9.7)	5.4 ± 0.9 (3.5–7.3)	5.6 ± 1.6 (3.2–8.9)	0.892
Distal pole, met. plate (μm)	6.1 ± 1.3 (1.4–9.2)	6.2 ± 1.4 (3.8–9.2)	5.8 ± 1.3 (1.4–7.9)	6.2 ± 1.3 (4.5–8.6)	0.377

Data are mean ± SD (range). Ivo, oocytes from simulated cycle matured *in vivo*; Igv, leftover cumulus-free GV oocytes from stimulated cycles matured *in-vitro*; ivm, immature cumulus-cell oocyte complexes recovered from *in vitro* maturation cycles and matured *in vitro*.

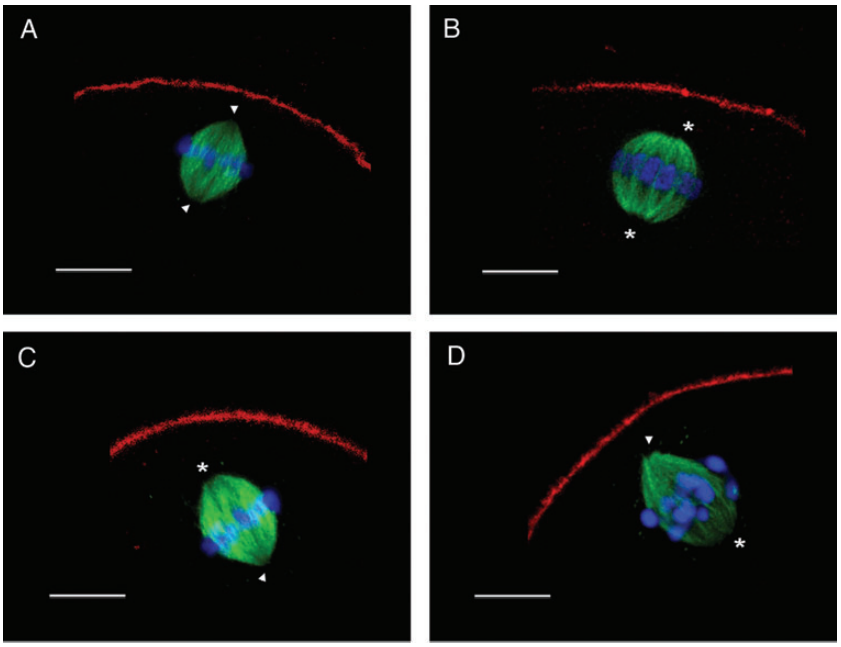

Figure 2 Three-dimensional reconstructions of MII spindles displaying different combinations of pole morphology. Microtubule tubulin is represented in green, chromosomes in blue and actin in red. Flattened poles (asterisks) were defined as ones having an overall size ≥2 μm, whereas focused poles (arrowheads) were defined as those having an overall size <2 μm. (**A**) Double focused, (**B**) double flattened, (**C**) flattened focused, with flattened pole near the oocyte surface and (**D**) focused flattened, with focused pole near the oocyte surface.

towards the oolemma was also positively correlated with a higher rate of chromosome displacement from the metaphase plate (70.6 versus 41.9, $P = 0.018$; data not shown in table).

With regard to spindle position relative to the oocyte surface, spindles with chromosomes regularly arranged on the metaphase plate showed a distance from the cortical actin comparable with that of spindles with one or more chromosome displaced along the major axis (7.0 ± 1.6 and 7.0 ± 1.1 μm, respectively; $P = 0.995$). Similarly, no difference in the distance from cortical actin was found between spindles with two regular rings outside and inside the spindle surface and spindles with a disorganized arrangement (6.9 ± 2.1 and 6.4 ± 0.9 μm, respectively; $P = 0.805$).

Regarding the microtubule density parameters, no statistically significant differences were detected between spindles with correct equatorial arrangement and those with imperfect chromosome congression, although in both distal and proximal hemidomains a trend towards a higher peak of maximum intensity was observed in spindles with chromosomes orderly arranged on the metaphase plate (Supplementary data, Table SI).

Impact of age

Within the samples available for analysis in this study, our attempts to evaluate the impact of maternal age were limited by the number of

Table II Spindle pole morphology in MII oocytes matured *in vivo* or *in vitro*.

Poles shape	All oocytes (%)	Oocyte category (%)			*P*
		ivo-MII	lgv-MII	ivm-MII	
Double flattened	31 (47.7)	11 (34.4)	16 (69.6)	4 (40.0)	0.095
Double focused	2 (3.1)	1 (3.1)	0 (0.0)	1 (10.0)	
Flattened focused, with flattened pole near the oocyte surface	3 (4.6)	2 (6.3)	1 (4.3)	0 (0.0)	
Focused flattened, with focused pole near the oocyte surface	29 (44.6)	18 (56.3)	6 (26.1)	5 (50.0)	

Ivo, oocytes from simulated cycle matured *in vivo*; lgv, leftover cumulus-free GV oocytes from stimulated cycles matured *in-vitro*; ivm, immature cumulus-cell oocyte complexes recovered from *in vitro* maturation cycles and matured *in vitro*.

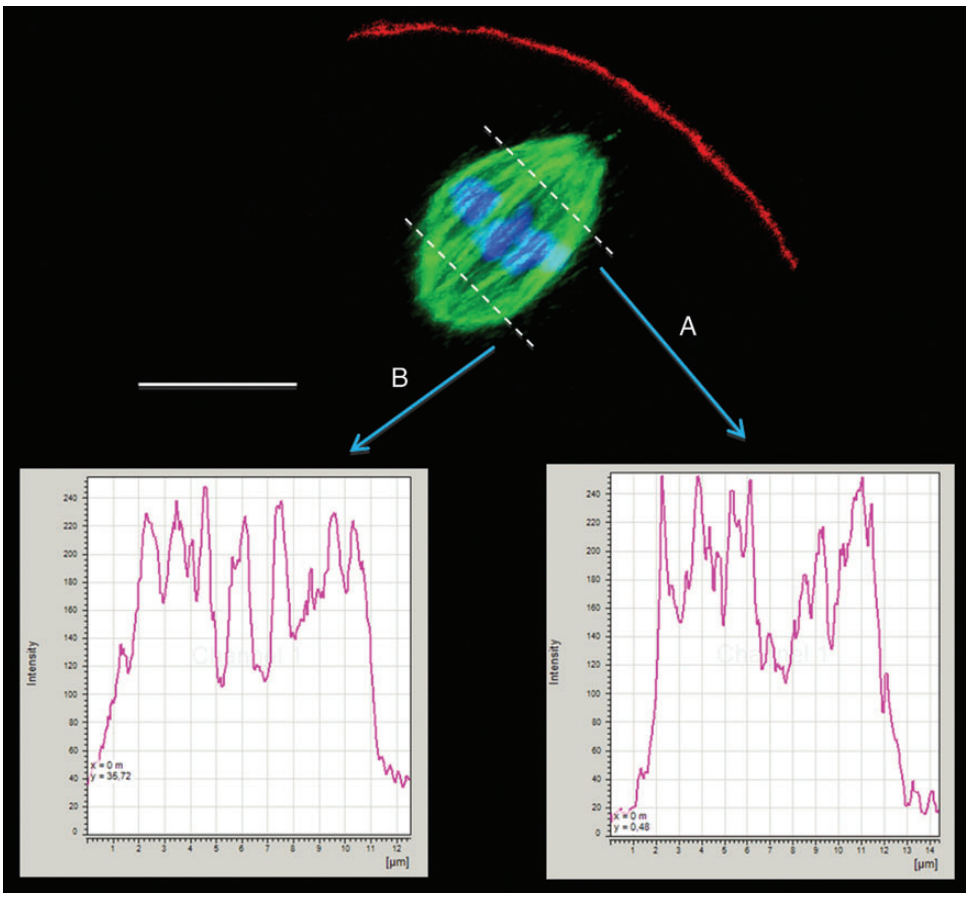

Figure 3 Optical intensity profiles for the tubulin channel (green) representing semi-quantitative measurements of microtubule abundance in an MII spindle three-dimensional reconstruction. Chromosomes and actin are represented in blue and red, respectively. Tubulin signal intensity was measured along two reference lines drawn transecting the spindle hemidomains, proximal (a) and distal (b) to the oocyte surface, in an intermediate position between the pole and the metaphase plate. Bar equals 10 µm.

samples in the age categories chosen for representation. To maximize sample numbers in these categories, we drew a cut-off value of <36 year for our youngest patients and one of >39 years for the oldest group recognizing that other age groupings have been used in the literature. To our knowledge, this grouping does represent the clinically recognized limits for age-related aneuploidy and we fully plan (ongoing studies) to enlarge this database for better age resolution in the future.

Although differences did not reach statistical significance, in ivo-MII spindles a marked trend was observed towards a progressively lower rate of spindles with correct chromosome alignment on the metaphase plate with increasing age (63, 43 and 25%, respectively). Conversely, in

Table III Microtubule abundance parameters in MII oocytes matured *in vivo* or *in vitro*.

Parameter	Oocyte category (no.)			*P*
	ivo-MII (32)	Igv-MII (23)	ivm-MII (10)	
Hemispindle proximal to the oocyte surface				
Maximum intensity	184.6 ± 56.8	157.3 ± 79.0	159.1 ± 56.0	0.267
Mean intensity	71.8 ± 28.8	84.1 ± 44.2	90.9 ± 66.5	0.360
Fibre intensity	19.0 ± 8.6	18.5 ± 11.1	24.6 ± 23.6	0.413
Hemispindle distal to the oocyte surface				
Maximum intensity	195.9 ± 45.6	161.6 ± 69.7	192.8 ± 39.2	0.071
Mean intensity	84.9 ± 36.8	100.9 ± 62.5	119.2 ± 70.3	0.176
Fibre intensity	23.4 ± 10.2	22.2 ± 10.8	29.5 ± 21.7	0.309

Ivo, oocytes from simulated cycle matured *in vivo*; Igv, leftover cumulus-free GV oocytes from stimulated cycles matured *in-vitro*; ivm, immature cumulus-cell oocyte complexes recovered from *in vitro* maturation cycles and matured *in vitro*.

Table IV Spindle morphometry and chromosome arrangement on the metaphase plate.

Parameter	Chromosome arrangement on the metaphase plate (no.)		*P*
	Regular (38)	At least one displaced chromosome (55)	
Major axis (μm)	11.3 ± 2.3 (7.2–18.4)	11.8 ± 2.3 (7.3–18.9)	0.163
Minor axis (μm)	8.9 ± 1.5 (5.9–12.9)	9.1 ± 1.6 (3.4–11.9)	0.275
Major/minor axis ratio	1.30 ± 0.28 (0.74–2.02)	1.34 ± 0.35 (0.78–2.81)	0.264
Maximum projection (μm^2)	86.6 ± 26.4 (41.8–167.9)	90.7 ± 25.6 (29.1–154.8)	0.229
Proximal pole, met. plate (μm)	5.4 ± 1.3 (3.2–9.7)	5.6 ± 1.4 (3.2–9.7)	0.258
Distal pole, met. plate (μm)	5.9 ± 1.4 (1.4–8.7)	6.2 ± 1.3 (3.8–9.2)	0.113

Data are mean ± SD (range).

Igv-MII the proportion of spindles with normal chromosome alignment did not exceed 25% in all age groups (Fig. 5). ivm-MII spindles were evaluated separately because not sufficiently represented or absent in the 36–39 and >39 years categories, respectively. However, in younger patients, these spindles displayed an incidence of normal chromosome alignment comparable with ivo-MII spindles (67%).

Morphometric (Supplementary data, Table S2) and microtubule density (Supplementary data, Table S3) parameters were not statistically different between samples of patients of different ages, with the exception of the major spindle axis, which was shorter in the <36 years group. However, a consistent decrease in all the microtubules density parameters in oocytes of patients >39 years suggests a clear direction for future studies.

Discussion

The microtubule cytoskeleton of the fully grown oocyte fulfils a fundamental role in the concluding stages of oogenesis, providing the structural framework for the two meiotic divisions. Vast information gained on the structure and function of the oocyte cytoskeleton in animal models has crucially contributed to the definition of general paradigms of female meiosis (Brunet and Verlhac, 2010; Evans and Robinson, 2011; Fabritius *et al.*, 2011). However, species-specific differences have not always allowed the extension of these findings to the human oocyte, leaving unanswered questions that have important practical and clinical implications. The present study was undertaken with the aim of obtaining novel details/attributes about the MII spindle of the human oocyte, thereby informing more systematic analyses for future investigations in this field. Our findings, summarized in Table VII (i) illustrate detailed morphometric and morphological properties, previously unrecognized, of the bipolar MII spindle; (ii) suggest that only a subset of these properties have some ability to predict a correct chromosome alignment on the metaphase plate; (iii) indicate that maturation *in vitro* of COCs obtained from IVM cycles does not affect the morphology of the meiotic spindle and chromosome alignment.

We trust that the observed spindle characteristics of the different oocyte types reflect genuine biological conditions, irrespective of the methodology adopted to fix and stain the microtubule apparatus. Concerning this, it should be noted that our immunostaining procedure used taxol. This agent is known to stabilize microtubules structures by preventing the dissociation of high-molecular-weight microtubule-associated proteins proteins and could theoretically induce microtubule polymerization. However, because exposure to taxol was simultaneous with detergent-facilitated formaldehyde fixation, the immediate access

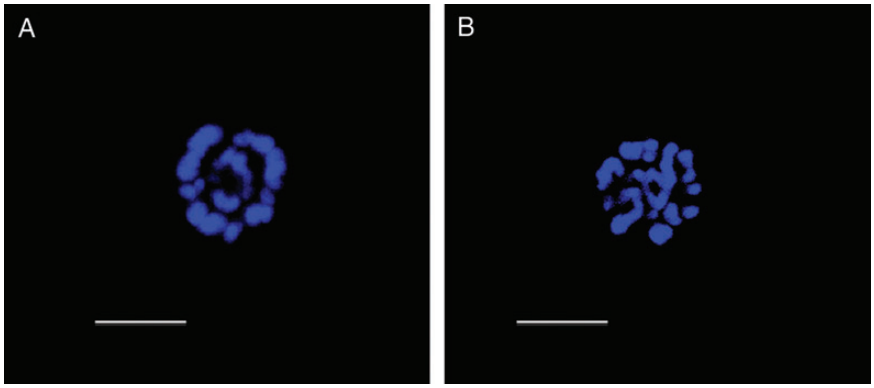

Figure 4 Alternative chromosome arrangements observed from an optical axis passing through the spindle poles encompassing (**A**) two regular rings organized outside and inside the spindle surface or (**B**) partially disorganized arrangement. For image clarity, the tubulin staining was omitted. Bar equals 10 μm.

Table V Spindle morphometry and chromosome arrangement inside–outside the spindle surface.

Parameter	Inside–outside chromosome arrangement (no.)		*P*
	Regular (21)	Disarranged (33)	
Major axis (μm)	11.2 ± 1.8 (7.2–14.4)	12.1 ± 2.2 (7.4–18.9)	0.062
Minor axis (μm)	9.0 ± 1.5 (6.3–12.9)	9.2 ± 1.2 (7.1–11.9)	0.309
Major/minor axis ratio	1.27 ± 0.28 (0.86–1.87)	1.33 ± 0.26 (0.90–2.02)	0.214
Maximum projection (μm^2)	85.9 ± 20.7 (47.1–122.8)	92.7 ± 20.7 (44.8–154.8)	0.121
Proximal pole, met. plate (μm)	5.3 ± 1.1 (3.2–8.0)	5.8 ± 1.3 (4.4–9.7)	0.061
Distal pole, met. plate (μm)	6.0 ± 1.1 (4.1–8.6)	6.2 ± 1.4 (1.4–9.2)	0.214

Data are mean ± SD (range).

of a protein cross linker during detergent-effected dilution of soluble protein is rather unlikely to have modified spindle structure as a result of this type of specimen preparation. This belief is also supported by the fact that MII spindles of *in vitro* matured murine oocytes were reported to be virtually identical in size and shape in two independent studies involving fixation protocols with or without taxol (Ibanez *et al.*, 2005a,b; Shen *et al.*, 2005).

Size and shape of the meiotic spindle

Morphometric analysis revealed that, irrespective of whether maturation occurs *in vivo* or *in vitro*, the size of the human MII spindle can be expressed by axial dimensions of ~12 × 9 μm. This finding raises puzzling questions if evaluated in comparison with the information available for the MII spindle of mouse oocytes, whose major axis ranges 20–30 μm, depending on maturation conditions (Sanfins *et al.*, 2003). Such a discrepancy is rather counter intuitive, considering the much smaller size (~80 μm) of the mouse oocyte. Furthermore, the larger spindle size observed in the mouse cannot be explained by a larger chromosome complement, which in comparison with the human is in fact smaller by both chromosome number and haploid DNA content. Interestingly, similar inconsistencies are observed also in the marmoset monkey, a non-human primate model, in which MII spindles with a major axis size of ~25 μm are found in oocytes of < 100 μm in diameter (Delimitreva *et al.*, 2012). Therefore, from a purely mechanistic standpoint, future studies will have to address the question of why a larger oocyte requires a smaller spindle, also elucidating the possible implications.

A novel aspect of our observations concerns the spindle shape. In several previous studies, MII spindles of human and non-human oocytes were considered normal when they showed a barrel-shaped organization (Rossi, 2006; Nichols *et al.*, 2010; Vieira *et al.*, 2010). However, this description conceals the fact that the spindle poles can be narrowly focused or flattened.

Discriminating the shape of the two poles on the basis of their proximity to the oocyte surface, we observed all the four combinations of poles morphology in individual spindles. It was noticed that double-focused spindles were marginally represented in our sample set, while almost all the spindles showed a profile with double-flattened or focused-flattened poles, in equivalent proportions. These frequencies are not easily explainable, but it is striking that they had a very similar patterns in all the three different classes of oocytes examined in our analysis.

Table VI Spindle pole morphology and chromosome arrangement on the metaphase plate.

Pole shape	Chromosome arrangement on the metaphase plate (%)		*P*
	Regular	At least one displaced chromosome	
Double flattened	11 (35.5)	20 (58.8)	0.017
Double focused	2 (6.5)	0 (0.0)	
Flattened focused, with flattened pole near the oocyte surface	0 (0.0)	3 (8.8)	
Focused flattened, with focused pole near the oocyte surface	18 (58.1)	11 (32.4)	

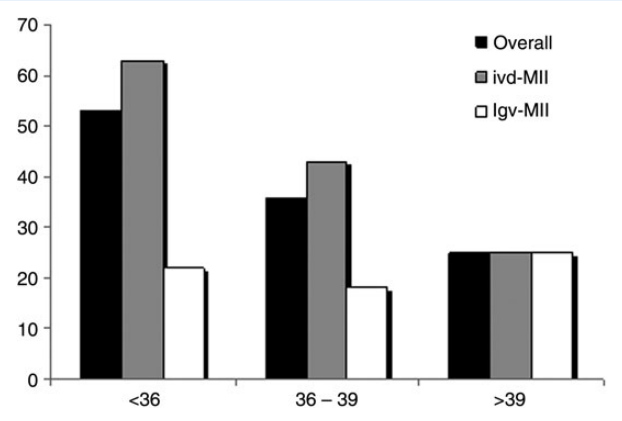

Figure 5 Percentages of spindles (*Y* axis) displaying normal chromosome arrangement in ivo-MII and Igv-MII oocytes obtained from women of three different age groups: <36, 37–39 and >39 years (*X* axis).

It was also intriguing to note that in spindles displaying both focused and flattened terminals, the focused pole was almost invariably oriented towards the oocyte cortex. The observation of different shapes of spindle poles is not merely anecdotal, but reflects important, although not fully appreciated, functional differences. For example, in mouse oocytes, spindles with focused or flattened poles can be observed in oocytes matured either *in vivo* or *in vitro*, respectively, and differ in the fact that in the former γ-tubulin it is restricted to the poles, while in the latter it is spread throughout the microtubular structure (Sanfins *et al.*, 2003). These findings are relevant, given the diminished quality of *in vitro* matured oocytes (Sanfins *et al.*, 2003), variations in spindle pole composition (Ibanez *et al.*, 2005a,b) and the differences that have been reported between meiotic spindles in human and mouse oocytes (Albertini *et al.*, 2003). We assessed pole shape without deliberately detecting specific pole markers, such as pericentrin or γ-tubulin. This was justified by the fact that in a previous study (Combelles *et al.*, 2002) we attempted to localize spindle pole markers in human oocytes after varying fixation conditions and found that traditional markers for centrosomal material are not organized at the spindle poles in this species as they are in somatic cells or the oocytes from other mammalian species. Importantly, we have routinely observed centrosome staining with both pericentrin and γ-tubulin antibodies in cumulus cells attached to the same oocytes, providing an internally controlled validation.

Spindle characteristics and chromosome arrangement

The question of a possible correlation between spindle size and chromosome arrangement has been only occasionally explored in previous studies. Chromosome misalignment has been described to occur as an effect of various intrinsic and extrinsic oocyte conditions, but there is no established notion on whether destabilization of chromosome organization may be reflected into or caused by alterations of the proportions of spindle bipolarity. The only direct analysis of this kind derived from the work of Bromfield *et al.*, (2009) who reported that in human oocytes the degree of chromosome scattering from the metaphase plate was positively associated with spindle length. Our data do not support the hypothesis that spindle size—expressed by major and minor axes, their ratio and maximum projection—is predictive of whether chromosomes are orderly arranged on the metaphase plate or subject to longitudinal (or indeed radial) displacement. This inconsistency may be only apparent. In fact, the evidence reported by Bromfield *et al.* (2009) concerned frozen–thawed oocytes in which energy-producing metabolism and, consequently, the forces that forge spindle shape may be altered (Jones *et al.*, 2004). During freezing–thawing, the MII spindle undergoes complete depolymerization, but it has the ability to recover bipolarity and chromosomes alignment by 1 h after thawing. However, over the following 3–4 h post-thawing, the spindle tends to elongate commensurate with chromosome displacement from the metaphase plate (Bromfield *et al.*, 2009). This loss of organization, secondary to an initial recovery, likely reflects reduced availability of energy stores caused by the response of the oocyte to the double insult of freezing and thawing. Energy, mainly in the form of GTP and ATP, is in fact necessary not only to support spindle formation and maintenance through tubulin polymerization, but also to determine spindle shape and chromosome position via the action of motor proteins (Zou *et al.*, 2008). This may explain why in frozen–thawed oocytes, in which energy depletion may cause perturbations of spindle and chromosome dynamics, a positive correlation between spindle length and chromosome displacement was observed, while in fresh oocytes, that are energetically non-compromised, a similar association did not emerge.

On the contrary, spindle pole organization seems to be correlated with chromosome spatial disposition. Loss of focusing at both poles appeared to be associated with higher chances of chromosome misalignment. Maintenance of at least one focused pole was positively correlated with correct chromosome alignment, provided that the focused pole was oriented towards the oocyte surface. These observations, while suggesting that normal chromosome arrangement is compatible with a certain

Table VII Summary of findings concerning spindle morphometry, spindle pole shape and microtubule abundance parameters in oocytes matured *in vivo* or *in vitro*.

Spindle morphometry parameters	Comparable between ivo-MII, lgv-MII and ivm-MII oocytes, except the major/minor axis ratio that is smaller in lgv oocytes
	Not predictive of chromosome alignment on the metaphase plate or inside–outside arrangement
	Major axis larger in oocytes of older women
Microtubule abundance parameters	Comparable between ivo-MII, lgv-MII and ivm-MII oocytes in both proximal and distal hemispindles
	Not predictive of chromosome alignment on the metaphase plate or inside–outside arrangement
	Trend towards smaller values with increasing woman's age
Pole shape	Both poles flattened positively associated with the displacement of one or more chromosomes from the metaphase plate
	Single or double focused poles positively associated with regular chromosome arrangement on the metaphase plate
Frequency of different pole shape combinations	Comparable between ivo-MII, lgv-MII and ivm-MII oocytes

degree of spindle asymmetry (i.e. loss of focusing at one pole), on the other hand lend credence to the idea that not only pole shape but also spindle polarity (i.e. orientation) may have a functional significance. In particular, it seems that proximity to the cortex coincides more frequently with a focused organization of the spindle pole and that this condition is more favourable for a correct chromosome alignment. Pole morphology has been investigated in experimental models, but our data cast a renewed interest in this subject for its relevance to chromosome arrangement, especially in consideration of a possible regulative role played by the cortex.

Cytoskeleton organization and age

Increased oocyte aneuploidy as an effect of maternal age, especially after the age of 35, is the single most important factor that affects human fertility and impacts the chromosomal integrity of the conceptus (Hunt and Hassold, 2008). Recent evidence generated in the mouse model indicates that such a phenomenon, occurring also in other mammals, derives from loss of cohesive proteins at the centromeric or recombination sites, leading to premature sister chromatid separation at meiosis I or II (Chiang *et al.*, 2010; Hunt and Hassold, 2010; Lister *et al.*, 2010; Jones and Lane, 2012). In the human, similar findings were recently reported (Duncan *et al.*, 2012). Preimplantation genetic screening studies also point towards a significant role for premature chromatid separation (Capalbo *et al.*, 2013). The human MII spindle has been the focus of research investigations on age-related meiotic aneuploidy, given its role in chromosome segregation during oocyte maturation. Previous observations revealed an increased chromosome longitudinal misalignment in MII spindles of oocytes of older women (Battaglia *et al.*, 1996). Our data confirm that normal chromosome alignment decreases with increasing maternal age in *in vivo* matured oocytes. GV-stage oocytes recovered from stimulated cycles and matured *in vitro* devoid of cumulus cells displayed spindles with high rates of chromosome misalignment in all the examined age classes, indicating that such material, especially if in association with cumulus cell-free maturation conditions, is inadequate to study oocyte meiosis. However, our studies show that the incidence of normal chromosome alignment in oocytes of younger women obtained from IVM cycles and matured *in vitro* while still enclosed in their cumulus cells was comparable with that of *in vivo* matured oocytes. By performing three-dimensional reconstructions, we were unable to ascertain systematically the constitution of misaligned chromatin masses, but at least in some cases the displaced chromosomes had the appearance of chromatid pairs, suggesting that, in addition to premature chromatid separation, other mechanisms are likely involved that would contribute to meiosis II malsegregation. In this context, our findings regarding microtubule abundance are relevant. Although no statistically significant differences in microtubule abundance were found between oocytes from different age groups, a decrease in fluorescence intensity was noticed in oocytes obtained from women >39. This finding prompts ongoing studies to test the hypothesis that increased maternal age may affect the mass and/or stability of microtubules in the MII spindle at a translational or post-translational level. Interestingly, one of the features that distinguishes human meiotic spindles from those of other mammals is the paucity of alpha subunit acetylation (Combelles *et al.*, 2002), a post-translational modification known to enhance microtubule stability. Collectively, our findings suggest that advanced maternal age may be influenced by a general weakening of protein–protein interactions that subserve important aspects of the cytoskeletal infrastructure required for chromosome alignment and mobility.

Comparison of the MII spindle of *in vivo* and *in vitro* matured oocytes

Many studies indicate that IVM profoundly affects the spindle dynamics and structure in human oocytes, thereby compromising the mechanism of chromosome segregation and enhancing the risk of aneuploidies in the conceptus (Cekleniak *et al.*, 2001; Delimitreva, 2005; Nichols *et al.*, 2010). As a consequence, clinical IVM is considered unsafe by many IVF specialists. We argue against this notion for several reasons. Firstly, the large majority of these studies adopted the mouse oocyte as a non-human model, whose cytoskeletal correlates are hugely different in comparison with the human (Albertini *et al.*, 2003). Secondly, nearly all human studies were based on the use of leftover GV-stage oocytes obtained from stimulated cycles and matured *in vitro* devoid of cumulus cells, corresponding to the lgv-MII typology of our work (Cekleniak *et al.*, 2001; Combelles *et al.*, 2002). This type of material is inappropriate for studying human IVM in many respects, mainly because the genomic integrity of such oocytes is intrinsically compromised (Guglielmo *et al.*,

2012), in addition to the fact that maturation *in vitro* in the absence of cumulus cells is a condition unquestionably incompatible with a correct unfolding of meiotic and cytoplasmic maturation (Sutton, 2003; Li and Albertini, 2013). Indeed, this is confirmed by the high incidence of chromosome misalignment observed in the present study, irrespective of maternal age. Thirdly, our evidence concerning the maturation of COCs recovered from IVM cycles uncovers morphological similarity between the cytoskeleton of *in vivo* and *in vitro* matured oocytes, including spindle size, pole shape, microtubule density and chromosome alignment. It should be noted, however, that we have not yet shown cytoplasmic competence in IVM oocytes and given the small sample sizes, some caution should be exercised regarding whether the traits identified at the level of spindle and chromosomes are valid indicators of oocyte quality. In addition, it should be noted that some of the observed spindle characteristics may reflect variations due to the degree of oocyte growth (i.e. size at the fully grown stage) after ovarian stimulation, which we previously reported does impact oocyte quality (Combelles *et al.*, 2002).

In conclusion, the present study provides novel insights into the mechanistic foundations of the spindle of the human oocyte, following maturation *in vivo* or *in vitro*. In availing biomarkers for a detailed analysis of the relationship between the microtubule scaffolding and chromosome organization, it is hoped that more informed approaches will be engaged in the areas of oocyte cryopreservation and IVM. Moreover, this work proposes new methodologies and themes for research on the human oocyte cytoskeleton, consistent with the overall aim of achieving a better definition of oocyte quality in human ART.

Supplementary data

Supplementary data are available at http://humrep.oxfordjournals.org/.

Acknowledgements

Part of this work was carried out at ALEMBIC, an advanced microscopy laboratory established by the San Raffaele Scientific Institute and the Vita-Salute San Raffaele University.

Authors' roles

G.C.: study design, coordination, manuscript drafting and critical discussion. M.C.G.: confocal microscopy, study design, laboratory tasks and critical discussion. M.D.C.: study design, laboratory tasks and critical discussion. F.B.: laboratory tasks and critical discussion. M.M.R.: study design, clinical tasks and critical discussion. E.D.P.: statistics, study design and critical discussion. R.F.: coordination, study design, clinical tasks and critical discussion. D.F.A.: confocal microscopy, study design and critical discussion.

Funding

Part of this work was supported by a grant awarded by the Italian Ministry of Labour, Health and Social Policies.

Conflict of interest

None declared.

References

Albertini DF, Sanfins A, Combelles CMH. Origins and manifestations of oocyte maturation competencies. *Reprod Biomed Online* 2003;**6**:410–415.

Battaglia DE, Goodwin P, Klein NA, Soules MR. Influence of maternal age on meiotic spindle assembly in oocytes from naturally cycling women. *Hum Reprod* 1996;**11**:2217–2222.

Bromfield JJ, Coticchio G, Hutt K, Sciajno R, Borini A, Albertini DF. Meiotic spindle dynamics in human oocytes following slow-cooling cryopreservation. *Hum Reprod* 2009;**24**:2114–2123.

Brunet S, Verlhac MH. Positioning to get out of meiosis: the asymmetry of division. Hum Reprod *Update* 2010;**17**:68–75.

Capalbo A, Bono S, Spizzichino L, Biricik A, Baldi M, Colamaria S, Ubaldi FM, Rienzi L, Fiorentino F. Sequential comprehensive chromosome analysis on polar bodies, blastomeres and trophoblast: insights into female meiotic errors and chromosomal segregation in the preimplantation window of embryo development. *Hum Reprod* 2013;**28**:509–518.

Cekleniak NA, Combelles CM, Ganz DA, Fung J, Albertini DF, Racowsky C. A novel system for *in vitro* maturation of human oocytes. *Fertil Steril* 2001; **75**:1185–1193.

Chiang T, Duncan FE, Schindler K, Schultz RM, Lampson MA. Evidence that weakened centromere cohesion is a leading cause of age-related aneuploidy in oocytes. *Curr Biol* 2010;**20**:1522–1528.

Combelles CMH, Cekleniak NA, Racowsky C, Albertini DF. *Assessment of nuclear and cytoplasmic* maturation in in-vitro matured human oocytes. *Hum Reprod* 2002;**17**:1006–1016.

Coticchio G. Sucrose concentration influences the rate of human oocytes with normal spindle and chromosome configurations after slow-cooling cryopreservation. *Hum Reprod* 2006;**21**:1771–1776.

Coticchio G, Bromfield JJ, Sciajno R, Gambardella A, Scaravelli G, Borini A, Albertini DF. Vitrification may increase the rate of chromosome misalignment in the metaphase II spindle of human mature oocytes. *Reprod Biomed Online* 2009;**19**(Suppl. 3):29–34.

Delimitreva S. Meiotic abnormalities in *in vitro*-matured marmoset monkey (Callithrix jacchus) oocytes: development of a non-human primate model to investigate causal factors. *Hum Reprod* 2005;**21**:240–247.

Delimitreva S, Tkachenko OY, Berenson A, Nayudu PL. Variations of chromatin, tubulin and actin structures in primate oocytes arrested during *in vitro* maturation and fertilization—what is this telling us about the relationships between cytoskeletal and chromatin meiotic defects? *Theriogenology* 2012;**77**:1297–1311.

Duncan FE, Hornick JE, Lampson MA, Schultz RM, Shea LD, Woodruff TK. Chromosome cohesion decreases in human eggs with advanced maternal age. *Aging Cell* 2012;**11**:1121–1124.

Evans JP, Robinson DN. The spatial and mechanical challenges of female meiosis. *Mol Reprod Dev* 2011;**78**:769–777.

Fabritius AS, Ellefson ML, McNally FJ. Nuclear and spindle positioning during oocyte meiosis. *Curr Opin in Cell Biol* 2011;**23**:78–84.

Fadini R, Brambillasca F, Renzini MM, Merola M, Comi R, De Ponti E, Dal Canto MB. Human oocyte cryopreservation: comparison between slow and ultrarapid methods. *Reprod Biomed Online* 2009;**19**:171–180.

Guglielmo M, Coticchio G, Albertini D, Dal Canto M, Brambillasca F, Lain M, Caliari I, Mignini Renzini M, Fadini R. DNA double strand breaks are associated with meiotic resumption failure in human GV-stage oocytes. *Hum Reprod* 2012;**27**(Suppl. 1):i189.

Hunt PA, Hassold TJ. Human female meiosis: what makes a good egg go bad? *Trends Genet* 2008;**24**:86–93.

Hunt P, Hassold T. Female meiosis: coming unglued with age. *Curr Biol* 2010; **20**:699–702.

Ibanez E, Sanfins A, Combelles CMH, overstrom EW, Albertini DF. Phenotype of mouse oocytes matured *in vivo* or *in vitro*. *Reproduction* 2005a;**130**:845–855.

Ibanez E, Sanfins A, Combelles CMH, Overstrom EW, Albertini DF. Genetic strain variations in the metaphase-II phenotype of mouse oocytes matured *in vivo* or *in vitro*. *Reproduction* 2005b;**130**:845–855.

Jones KT, Lane SIR. Chromosomal, metabolic, environmental, and hormonal origins of aneuploidy in mammalian oocytes. *Exp Cell Res* 2012; **318**:1394–1399.

Jones A, Van Blerkom J, Davis P, Toledo AA. Cryopreservation of metaphase II human oocytes effects mitochondrial membrane potential: implications for developmental competence. *Hum Reprod* 2004; **19**:1861–1866.

Li R, Albertini DF. The road to maturation: somatic cell interaction and self-organization of the mammalian oocyte. *Nat Rev Mol Cell Biol* 2013; **14**:141–152.

Lister LM, Kouznetsova A, Hyslop LA, Kalleas D, Pace SL, Barel JC, Nathan A, Floros V, Adelfalk C, Watanabe Y *et al.* Age-related meiotic segregation errors in mammalian oocytes are preceded by depletion of cohesin and Sgo2. *Curr Biol* 2010;**20**:1511–1521.

Nichols SM, Gierbolini L, Gonzalez-Martinez JA, Bavister BD. Effects of *in vitro* maturation and age on oocyte quality in the rhesus macaque *Macaca mulatta*. *Fertil Steril* 2010;**93**:1591–1600.

Pickering SJ, Johnson MH. The influence of cooling on the organization of the meiotic spindle of the mouse oocyte. *Hum Reprod* 1987;**2**: 207–216.

Rossi G. Meiotic spindle configuration is differentially influenced by FSH and epidermal growth factor during *in vitro* maturation of mouse oocytes. *Hum Reprod* 2006;**21**:1765–1770.

Sanfins A, Lee GY, Plancha CE, Overstrom EW, Albertini DF. Distinctions in meiotic spindle structure and assembly during *in vitro* and *in vivo* maturation of mouse oocytes. *Biol Reprod* 2003;**69**:2059–2067.

Shen Y, Betzendahl I, Sun F, Tinneberg H, Eichenlaub-Ritter U. Non-invasive method to assess genotoxicity of nocodazole interfering with spindle formation in mammalian oocytes. *Reprod Toxicol* 2005;**19**:459–471.

Sutton ML. Effects of in-vivo and in-vitro environments on the metabolism of the cumulus–oocyte complex and its influence on oocyte developmental capacity. *Hum Reprod Update* 2003;**9**:35–48.

Vieira RC, Barcelos ID, Ferreira EM, Martins WP, Ferriani RA, Navarro PA. Spindle and chromosome configurations of *in vitro*-matured oocytes from polycystic ovary syndrome and ovulatory infertile women: a pilot study. *J Assist Reprod Genet* 2010;**28**:15–21.

Wang W-H, Meng L, Hackett RJ, Oldenbourg R, Keefe DL. Rigorous thermal control during intracytoplasmic sperm injection stabilizes the meiotic spindle and improves fertilization and pregnancy rates. *Fertil Steril* 2002; **77**:1274–1277.

Zou J, Hallen MA, Yankel CD, Endow SA. A microtubule-destabilizing kinesin motor regulates spindle length and anchoring in oocytes. *J Cell Biol* 2008; **180**:459–466.